Theor Chem Acc (2009) 123:3–10
DOI 10.1007/s00214-009-0553-9

REGULAR ARTICLE

Ab initio study of the singlet-triplet splitting in reduced polyoxometalates

Coen de Graaf · Rosa Caballol · Susanna Romo · Josep M. Poblet

Received: 24 February 2009 / Accepted: 26 February 2009 / Published online: 18 March 2009

Abstract A valence bond analysis of the wave function of doubly reduced polyoxometales is presented, using the M_6O_{19} Lindqvist structure as test case. By a unitary transformation of the delocalised valence orbitals to localised metal centred orbitals, the multiconfigurational wave function is mapped onto a valence bond function with three different types of configurations: the two electrons are on the same site, on neighbouring sites, or on next-nearest neighbour sites. The inspection of the relative weights of these configurations for triplet and singlet state shows that the triplet-coupled electrons are confined to a smaller volume, and hence have a higher energy than the singlet-coupled electrons. This is in line with the experimental observation that the doubly reduced polyoxometalates show non-mangetic behaviour.

Keywords Polyoxometalates · Valence bond · magnetic interactions · DDCI

1 Introduction

Polyoxometalates (POM) form an interesting class of compounds with applications in many fields such as catalysis, material science and medicine [1]. Usually these polynuclear metal-oxygen clusters are formed by Mo, W or V atoms surrounded by six oxygens in a distorted octahedral coordination. The different ways to connect these MO_6 building blocks gives rise to a wide variety of structures ranging from a relatively small cluster (M_6O_{19}, the so-called Lindqvist complex, see Fig. 1) to nanostructures containing hundreds of metal atoms [2, 3].

An interesting feature of POMs is the ability to accept electrons without suffering large geometrical distortions or the decomposition of the complex. Depending on the nature of the metal ions in the cluster, these extra electrons can be localised on just one metal centre or either have a delocalised character. In a prototype POM structure such as the Keggin ion ($[XM_{12}O_{40}]^{m-}$, M = Mo, W; X = P, Si, Al, etc.), the extra electrons delocalise over all 12 metal ions. However, in substituted Keggin complexes, obtained by replacing Mo or W ions by V, the extra electrons localise preferentially on the V ion.

Electron spin resonance (ESR) spectra of one-electron reduced paramagnetic anions consist of very broad lines at room temperature, which narrow upon cooling. These observations have been interpreted as a result of delocalisation via hopping mechanism of the electron at high temperatures that becomes trapped at low temperatures. From the temperature variation of the ESR spectra it is accepted that electron delocalisation appears above 35 K for $[SiW_{12}O_{40}]^{5-}$ and 40K $[PMo_{12}O_{40}]^{4-}$ [4]. At room temperature the extra electron in the monoreduced α-Keggin anion is equally distributed (by hopping mechanism) over all the metal centres. Despite that one would expect the addition of a second electron to a highly symmetric structure should result in an increment in the magnetic moment, it is experimentally well established that reduced species with an even number of delocalised

Dedicated to Professor Santiago Olivella on the occasion of his 65th birthday and published as part of the Olivella Festschrift Issue.

C. de Graaf (✉) · R. Caballol · S. Romo · J. M. Poblet
Departament de Química Física i Inorgànica,
Universitat Rovira i Virgili,
Marcel lí Domingo s/n, 43007 Tarragona, Spain
e-mail: coen.degraaf@urv.net

C. de Graaf
Institució Catalana de Recerca i Estudis Avançats (ICREA),
Passeig Lluis Companys 23, 08010 Barcelona, Spain

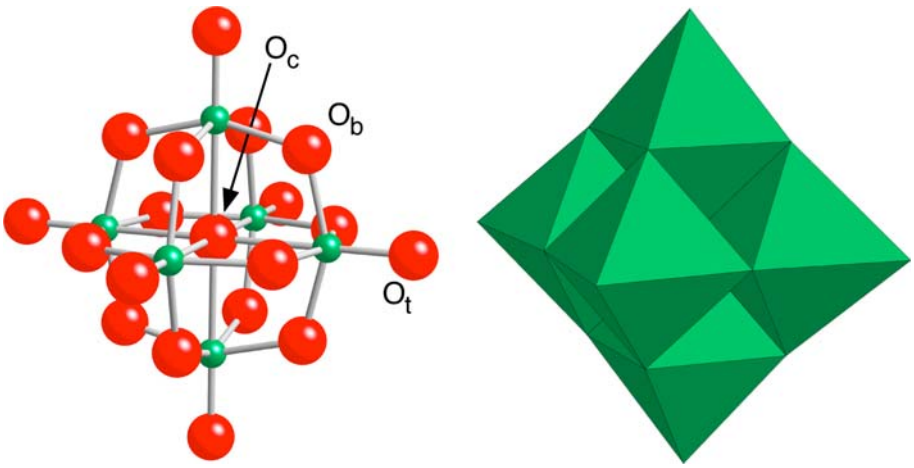

Fig. 1 Ball and stick representation (*left*) and polyhedral representation of the Lindqvist complex TM_6O_{19}. *Green spheres* represent Mo or W, *red* is O

electrons show diamagnetism [5, 6]. Based on theoretical studies, it is argued that the electrons pair up in a delocalised molecular orbital, in contrast to a paramagnetic situation in which the electrons are (anti-)ferromagnetically coupled and occupy different molecular orbitals. The latter type of behaviour can be found in substituted POMs such as the capped Keggin complexes $[PMo_{12}O_{40}(VO)_2]^{5-}$ or $[PMo_8V_4O_{40}(VO)_4]^{5-}$, where (part of) the extra electrons are localised on the V sites.

There exist by now a large number of density functional theory (DFT)-based studies of the electronic structure of POMs. These studies rationalised many important features such as the redox properties, protonation processes, etc. [7–11]. However, additional insight to the electronic structure can in principle be obtained from post Hartree-Fock (HF) methods by analyzing the *N*-electron wave function. The application of these wave function based methods is not straightforward given the large number of atoms even in the smallest POM. An interesting procedure to obtain detailed, accurate information was presented by Suaud and co-workers [12–15], who extracted effective interaction parameters through large configuration interaction calculations dividing the whole structure in fragments. The fragments contain two or four metal ions and all the oxygens bonded to these metals. Typical effective interactions are the hopping probability of an electron to a neighboring site (t) or the magnetic interaction between two electrons at neighboring sites (J). Once all important interactions have been parametrised, an effective Hamiltonian can be constructed for the whole molecule, and information can be obtained of the electronic structure of the complete structure. The application of this strategy to the doubly reduced Keggin ion provided an explanation of the diamagnetic character of this species in terms of hopping parameters, on-site repulsion and magnetic coupling strength.

Here, we address the same question but with a slightly different strategy. We concentrate on the electronic structure of the whole structure and subsequently map the multiconfigurational wave function onto a valence bond (VB) representation including all possible electron distributions over the metal centres. The comparison of the importance of the different electron arrangements in the diamagnetic singlet ground state and the excited triplet, representing the ferromagnetic solution, may give additional information about the mechanism that stabilises the singlet state. Being a rather time-consuming approach, we apply the strategy to the Lindqvist molecule as a proof of principle. Extension to the more interesting Keggin structure is in principle possible having the proper computer resources at hand.

2 Methodology

The application of wave function based methods to calculate the electronic structure of POMs requires a relatively cheap yet accurate computational scheme. Here, we apply the well established complete active space self consistent field (CASSCF) approach followed by either complete active space second-order perturbation theory (CASPT2) [16] or difference dedicated configuration interaction (DDCI) [17]. Provided an appropriate active space has been chosen, CASSCF accounts for all the important non-dynamical electron correlation effects, i.e., the admixture of all low energy electron configurations to the Hartree-Fock determinant. In most cases, the CASSCF wave function gives a rather accurate electron distribution but often fails to describe the relative energies of the different electronic states. For this purpose, dynamical electron correlation effects need to be included in the wave function. CASPT2 takes the CASSCF wave function as reference and estimates the effects of all single and double excitations on top of this wave function (see Fig. 2) by second-order perturbation theory. The zeroth-order

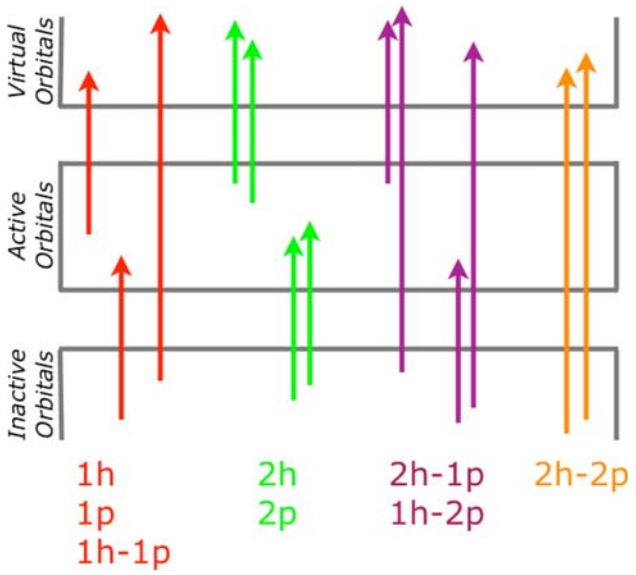

Fig. 2 Schematic representation of the excitations outside the CAS included in the CASPT2 and DDCI treatment of the dynamical electron correlation effects. The different classes of excitations are labelled by the number of holes (h) created in the inactive orbitals and particles (p) created in the virtual orbitals. The $2h$–$2p$ excitations are discarded in the DDCI approach

Hamiltonian is a Fock-type operator that reduces to the Møller-Plesset zeroth-order Hamiltonian for zero active orbitals. DDCI is a multireference CI strategy designed to calculate energy differences between electronic states rather than accurate total energies. All double excitations not involving any active orbital are eliminated from the CI space. This is based on the understanding that up to second-order perturbation theory, the $2h$–$2p$ class of excitations (see Fig. 2) gives a uniform shift of the diagonal matrix elements of the CI matrix, and hence, do not affect the relative energies of the different electronic states.

Despite its popularity in the first decades of quantum chemistry, Valence Bond (VB) theory is nowadays almost completely replaced by Molecular Orbital (MO) theory. In a recent historical overview of the rivalry of MO versus VB theory [18], the reasons for this decline were described, but it was also remarked that VB theory is slowly gaining some terrain again and continues to be a very powerful tool [19–29], especially for analysis purposes. Calculations described in this article are all done in the MO theory implementation of quantum chemistry, but the analysis of the wave function is done in VB terminology. This is done by a unitary transformation of the delocalised MOs into atomic-like orbitals and subsequently re-expressing the multiconfigurational wave function in the so-obtained localised orbitals. There exist many different orbital localisation schemes, and here we opt for the projection scheme described by Bordas et al. [30] in their study of the magnetic coupling in systems with elevated spin moments. A unitary transformation of the active orbitals is performed by the projection of a model vector $|\tilde{a}\rangle$ of pure M-3d_{xy} character in the active space. The model vector is localised on one metal centre and has non-bonding character, perpendicular to the M=O_t bond.

$$|a\rangle = \hat{P}|\tilde{a}\rangle = \left[\sum_{b}^{n} |b\rangle\langle b|\right]|\tilde{a}\rangle \quad (1)$$

with $|b\rangle$ an active natural orbital and n the total number of active orbitals. This projection process is repeated for six model vectors, each localised on a different metal.

2.1 Computational details

To optimise the geometries of the species considered in this study, we performed DFT-based calculations applying the Becke-Perdew 86 (PB86) [31–34] expression for the exchange-correlation functional as implemented in the ADF code [35, 36]. A Slater-type orbitals (STO) basis set of triple ζ + polarisation (TZP) quality was applied for the valence electrons. The core electrons were frozen and described by core potentials generated with the DIRAC program. For comparison purposes, we also performed B3LYP [37, 38] and BP86 calculations with Turbomole [39, 40] using a Gaussian-type orbitals (GTO) basis set of (TZP) quality.

The CASSCF/CASPT2 calculations have been performed with MOLCAS [41], the DDCI calculations with the CASDI program [42]. The LANL2 effective core potentials were used to described the Mo-[Ar,3d] and W-[Kr,4d,4f] core electrons. Valence electrons are described with the corresponding double ζ (DZ) basis set, although some test calculations have also been performed with larger basis sets, namely the TZP basis of Ahlrichs [43] applied in the B3LYP calculations and an all-electron TZP basis set of the atomic natural orbital-type [44]. The size of the active spaces used in the calculations will be commented for each application in the Sect. 3.

The W_6 and Mo_6 molecules transform following the symmetry rules of the O_h point group. Imposing this symmetry restrictions in the calculations would, however, not allow to transform the natural orbitals to localised atomic-like orbitals. Therefore, we performed the calculations without symmetry. The mono-substituted VW_5 and VMo_5 have C_{4v} symmetry. Due to the fact that only Abelian symmetry is implemented in MOLCAS, the calculations for these molecules were done in the C_{2v} point group. All wave function based calculations are performed at the DFT/BP86 optimised geometry.

3 Results

The comparison of theoretical values to X-ray data in Table 1 confirms the ability of the DFT/BP86 calculations

Table 1 Selected distances (in Å) and angles (in degrees) for $[M_6O_{19}]^{2-}$ and $[VM_5O_{19}]^{3-}$ (M = Mo, W) obtained by DFT/BP86 geometry optimisation

	$M–O_c$	$M–O_b$	$M–O_t$	$V–O_c–M$
$[Mo_6O_{19}]^{2-}$				
BP86	2.334	1.955	1.729	90
X-ray [46]	2.312–2.324	1.88–1.96	1.671–1.678	90
$[W_6O_{19}]^{2-}$				
BP86	2.337	1.942	1.730	90
X-ray [47]	2.33	1.92	1.69	90
$[VMo_5O_{19}]^{3-}$				
BP86	2.363	1.918	1.626	88.0
X-ray [48]	2.337	1.912	1.634	–
$[VW_5O_{19}]^{3-}$				
BP86	2.387	1.920	1.622	87.7
X-ray [45]	2.296	1.964	1.688	–

Results are compared to experimental data

to provide accurate estimates of the geometries of (substituted) POMs. The overall agreement with experimental data is similar to what is reported for related structures [9], in which the largest deviations between experimental and theoretical geometries are, in general, for the terminal W=O and Mo=O bonds. The computed V=O bond lengths of $\sim$1.62 Å for anions VMo_5 and VW_5 excellently agree with the experimental distance reported for VMo_5 anion (1.634 Å), but it is somewhat shorter than the reported bond length of 1.688 Å for the VW_5 anion. However, in the X-ray characterisation of the latter anion the occupancy of the vanadium atoms was randomly distributed on the three independent metallic sites of the polyanion, therefore the value of 1.688 Å [45] obtained from the X-ray structure corresponds to an average V=O and W=O distance. In fact, an accurate search in the Cambridge Structural Database shows that the terminal V=O bond lengths in vanadotungstates and vandomolybdates vary between 1.60 and 1.65 Å, values that plainly agree with the computed values.

Before analyzing the mechanism of spin pairing in doubly reduced POMs, we first focus our attention on the redox properties of mono-substituted Lindqvist structures. After replacing one of the W or Mo ions (with a formal charge of +6) by a V ion (formal charge +5), the $[VMo_5O_{19}]^{3-}$ or $[VW_5O_{19}]^{3-}$ (VMo_5, VW_5) complex can be reduced in two different ways. The extra electron can either localise on the V-site or become delocalised over the remaining five Mo ions. From experimental data and computational studies on other POMs, it is known that the situation with the extra electron localised on the more electronegative V-site is in general more favourable than a delocalised electron [9].

Table 2 lists the energy difference between reducing in the V-site and the five Mo-sites. Positive energies mean that the V-site is preferred. We compare the restricted open-shell HF (ROHF) and CASPT2 results with those obtained with the B3LYP or BP86 functionals. The B3LYP and BP86 calculations with Gaussian type orbitals (GTO) were done with Turbomole. The CASSCF reference wave function was constructed from a minimal active space that contains two orbitals: a V-3d_{xy} non-bonding orbital and a molecular orbital, i.e., a linear combination of the five Mo/W-3d_{xy} orbitals (the subindices refer here to a local coordination frame, where the z-axis is along the M-O_t bond). The orbitals are optimised for the average of the two states of interest.

Table 2 ROHF, DFT and CASPT2 estimates of the difference in the reduction energy (in kcal/mol) for V and Mo or W in VMo_5-1e and VW_5-1e

	ROHF	B3LYP	CASPT2	BP86 (GTO)	BP86 (STO)
VMo_5-1e	93	20	10	7	6
VW_5-1e	131	34	30	18	18

It is clear that all methods reproduce the expected behaviour, i.e. the first reduction of the mono-substituted Lindqvist structure occurs at the V-site (see Table 2). Whereas ROHF gives a very large energy difference between localised and delocalised solutions, the CASPT2 and different DFT estimates are in reasonable agreement with each other. The CASPT2 result is stable against changes in the one-electron basis set and also the extension of the active space beyond the minimal active space does not significantly affect the relative energies listed in the table. Furthermore, the larger energy difference between localised and delocalised solutions in the tungsten Lindqvist can be ascribed to larger difference in electronegativity between V and W than for V and Mo.

We now return to the non-substituted Lindqvist complexes to study the mechanism for the electron pairing in the doubly reduced species. The electronic structure of the

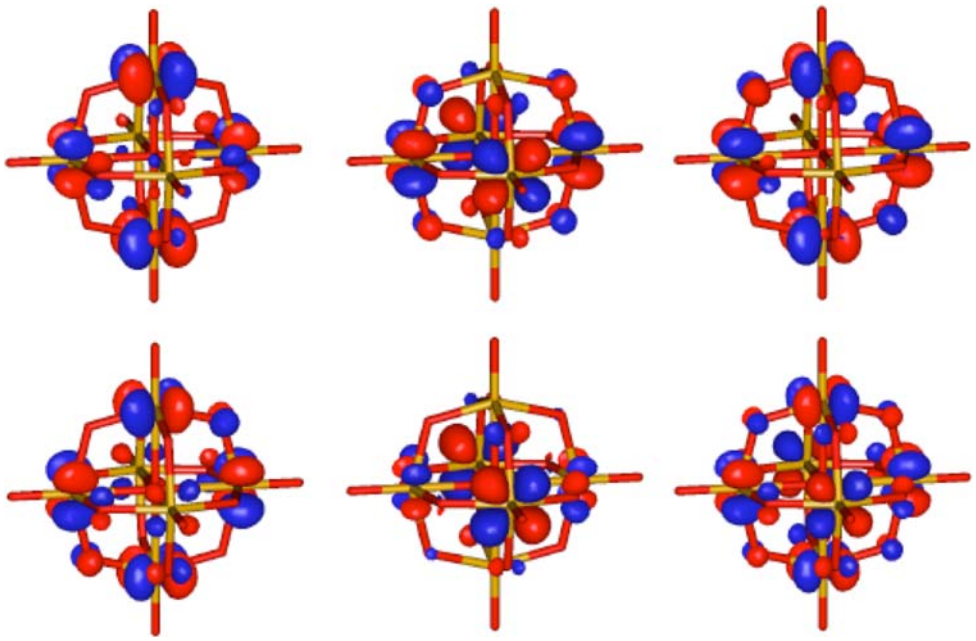

Fig. 3 CAS(2,6)SCF natural active orbitals for W_6-2e

fully oxidised species is relatively simple and is characterised by a set of highest occupied MOs of mainly oxygen character and at higher orbital energy a collection of unoccupied orbitals of mainly M-3d_{xy} character. Taking into account the overall octahedral symmetry of the molecule, six linear combination of these M-3d_{xy} orbitals can be formed that transform as the e_u, t_{2g}, and a_{2u} irreducible representations of the O_h symmetry point group. From these the e_u has the lowest orbital energy in the fully oxidised species. Following a simple one-electron reasoning, it can be argued that the two electrons added to the molecule in the double reduction process will occupy these e_u orbitals. Hence, the minimal active space to study the energy difference between the non-magnetic singlet and ferromagnetic triplet contains two orbitals and the two extra electrons. However, the t_{2g} and a_{2u} have just slightly higher orbital energies, and hence, it cannot be excluded that electronic configurations in which these orbital are occupied play an important role in the *N*-electron wave function.

The simple CAS(2,2)SCF calculation for W_6-2e gives an singlet-triplet energy difference (ΔE_{ST}) of −1.8 eV, while the subsequent CASPT2 treatment of the remaining electron correlation inverts the stability and gives ΔE_{ST} = 1.6 eV. Apart from this large change in relative energies, there are two related indications that make suspicious the result based on the minimal active space. In the first place, the weight of the CASSCF wave function in the first-order corrected wave function is significantly lower for the singlet than for the triplet. Second, there appear large contributions in the second-order estimate of the energy from configurations outside the CAS. Inspection of the character of these excitations learns that they are related to the occupation of the low-lying linear combinations of non-bonding M-3d_{xy} orbitals of t_{2g} and a_{2u} symmetry.

Table 3 CAS(2,6)SCF, CASPT2 and DDCI energy difference (in eV) between the lowest singlet and triplet states of Mo_6-2e and W_6-2e

	CASSCF	CASPT2	DDCI
Mo_6-2e	0.72	0.26	0.32
W_6-2e	0.61	0.12	0.33

The optimised natural orbitals that result from the extension of the active space with the t_{2g} and a_{2u} are shown in Fig. 3. The singlet state indeed has a large multiconfigurational character. The e_u^2 electronic configuration has a weight of approximately 66%, the t_{2g}^2 configuration accounts for about 33%, and the a_{2u}^2 configuration is less important. The weight of this extended CASSCF wave function in the corrected singlet wave function is now practically equal to the weight in the triplet. Moreover, there are no large contributions to the second-order energy anymore. The results in Table 3 show that both the variational and perturbative treatments of the dynamical electron correlation lead to similar values for ΔE_{ST}, while CAS(2,6)SCF seems to overestimate the stability of the singlet state.

The relatively large singlet-triplet energy gap (∼0.3 eV) is consistent with diamagnetism reported for doubly reduced tungstates and molybdates [6]. An energy gap of 0.78 eV was found for the decatungstate $[W_{10}O_{32}]^{6-}$ combining a phenomenological Hamiltonian and *ab initio* calculations on fragments [49].

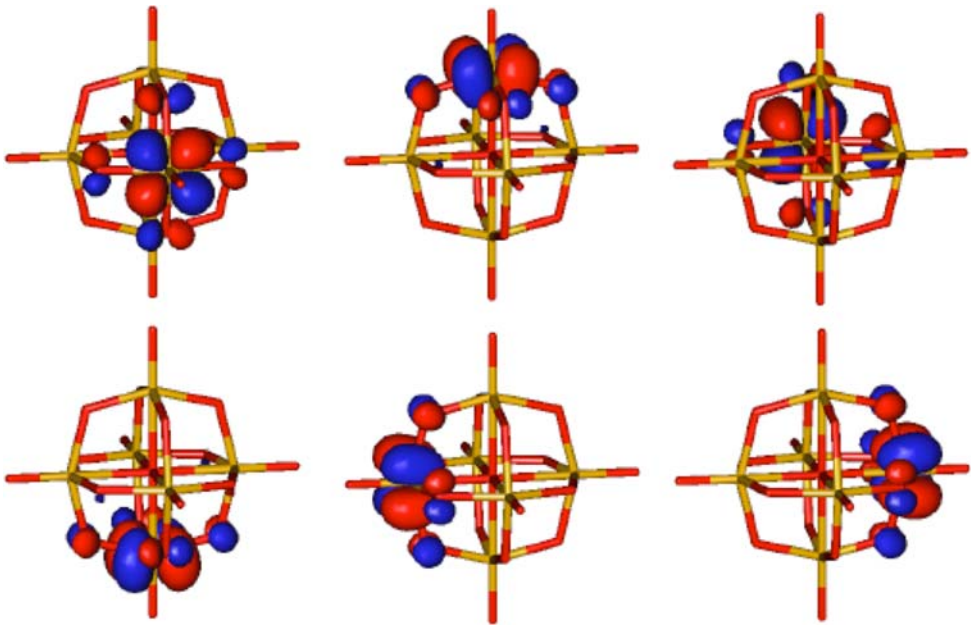

Fig. 4 Localised atomic-like orbitals for W_6-2e

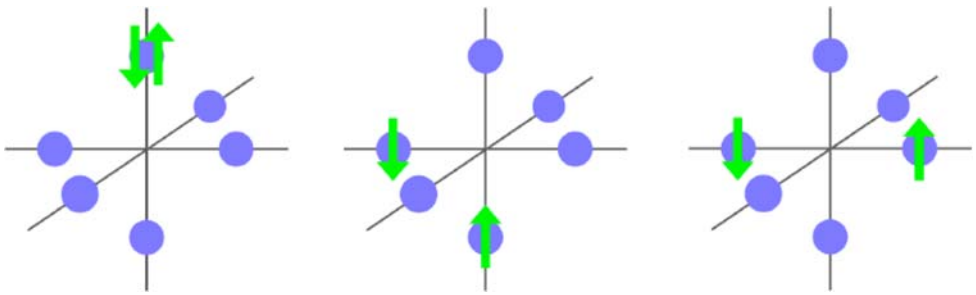

Fig. 5 Schematic representation of the VB configurations considered in the analysis of the *N*-electron wave function of the doubly reduced Lindqvist complex. From *left* to *right*, on-site, nearest neighbour (NN) and next-nearest neighbour (NNN) configurations

3.1 Valence Bond analysis

By the projection of model vectors onto the active space, the delocalised natural orbitals were transformed in localised atomic-like orbitals as shown in Fig. 4. The method is described in Ref. [30] for projection into the inactive molecular orbital space and has been adopted in the course of this study to be applied for active orbitals. Since the wave function is a complete CI expansion in the active space, the transformation of the active orbitals leaves the electron distribution unchanged and does not affect the energy of the system. In many Valence Bond implementations, the different configurations can overlap and in the determination of the weight of the different VB configurations one has to account for this overlap. The here-applied projection method results in local orbitals that are mutually orthogonal and by construction also orthogonal to the inactive and virtual orbitals. Recently, Malrieu and co-workers published an interesting account on the advantages of the use of orthogonal localised orbitals in the VB analysis of the wave function [50].

For the W_6-2e and Mo_6-2e systems, the singlet wave function expressed in local orbitals contains three different types of VB configurations. Figure 5 shows how the two extra electrons can occupy orbitals localised on next-nearest neighbours (NNN), on nearest neighbours (NN), and finally, the two electrons can be on one metal site, occupying the same orbital (on-site). This configuration is of course not possible for the triplet wave function.

Casañ-Pastor and Baker [6] already suggested from experiments that although the two extra electrons in doubly reduced tungstates are firmly and completely coupled antiferromagnetically, it must not be concluded that they permanently reside on adjacent W atoms. Table 4 lists the weights of the VB configurations for the singlet and triplet electronic states. As expected, the dominant configuration for both electronic states corresponds to the one where the electrons are on the opposite sides of the molecule. The weight of the NNN configuration is larger in the triplet than in the singlet, while this is inverted for the NN configurations. In combination with the fact that the electrons even have small probability to be found on the same atom, it can

Table 4 Weights (in %) of the on-site, nearest-neighbour (NN) and next-nearest-neighbour (NNN) VB configurations in the CAS(2,6)SCF wave function for the lowest triplet and singlet states of the doubly reduced Lindqvist complex W_6-2e

	On-site	NN	NNN
Singlet	0.9	20.2	78.6
Triplet	–	13.4	86.5

be concluded that the singlet-coupled electrons can approach each other more, and hence, occupy a larger volume. On the contrary, the triplet-coupled electrons occupy a smaller region in space and their movement is more restricted than in the singlet state. This leads to an extra stabilisation of the singlet state with respect to the triplet state. A similar conclusion was extracted from the model Hamiltonian study of the Keggin ion by Suaud et al., who concluded that the hopping processes are more effective for the singlet than the triplet states.

4 Summary and conclusions

The study of the electronic structure of (small) POMs through multiconfigurational wave function based computational schemes is within reach and can add additional insight to the more widely applied DFT-based calculations. This is especially true when the electronic structure counts with unpaired electrons that show complex magnetic coupling patterns.

For the mono-substituted Lindqvist complexes (VM_5O_{19}; M = Mo or W), we estimate by CASSCF calculations followed by CASPT2 or DDCI that the reduction of the cage at the V-site is favoured by about 10 kcal/mol with respect to the Mo and by 30 kcal/mol with respect to W. This values are comparable to those obtained with DFT/B3LYP calculations. A comparison with experimental data would of course require the inclusion of solvent effects and the calculation of a second reduction energy, since a selective reduction on either V or Mo/W cannot be performed experimentally. Such strategy has recently been applied for larger POMs resulting in a rather accurate description of the multiple reduction processes observed in experiment.

The diamagnetic character of the doubly reduced Lindqvist species Mo_6O_{19} and W_6O_{19} was studied by mapping the multiconfigurational wave function onto a valence bond wave function containing three types of electronic configurations. It was shown that the electronic configuration with the electrons on opposite sides of the molecules is the most important, but significant contributions arise from the configurations with the two electrons on neighbouring sites. This contribution is more important for the singlet than for the triplet, and hence, it is concluded that the presence of an electron on centre '*a*' restricts the other electron to a smaller volume in the triplet than in the singlet function. This indicates that the difference in the efficiency of the delocalisation process is at the origin of the observed diamagnetic character of the doubly reduced POMs.

Acknowledgments Prof. Santiago Olivella has been a reference for various generations of Spanish quantum chemists for his scientific rigour and for generously sharing his broad knowledge. It has been a privilege to receive his advices and to collaborate with him. Financial support has been provided by the Spanish Ministry of Education and Science (Projects CTQ2005-06909-C02-01/BQU and CTQU2005-08459-C02-02/BQU), and the Generalitat de Catalunya (Project 2005SGR-00104). Our group belongs to the "Theoretical and Computational Chemistry Network (*Xarxa d'R+D+I en Química Teòrica i Computacional, XRQTC*) supported by the Generalitat de Catalunya.

References

1. Katsoulis DE (1998) Chem Rev 98:359
2. Kortz U, Hussain F, Reicke M (2005) Angew Chem Int Ed 44:3773
3. Müller A, Das SK, Talismanova MO, Bögge H, Kögerler P, Schmidtman M, Talismanov SS, Luban M, Krickemeyer E (2002) Angew Chem Int Ed 41:579
4. Sanchez C, Livage J, Launay JP, Fournier M, Jeannin Y (1982) J Am Chem Soc 104:3194
5. Kozik M, Casañ-Pastor N, Hammer CF (1988) J Am Chem Soc 110:7697
6. Casañ-Pastor N, Baker LCW (1992) J Am Chem Soc 114:10384
7. Rohmer M-M, Bénard M, Blaudeau J-P, Maestre JM, Poblet JM (1998) Coord Chem Rev 178–180:1019
8. López X, Bo C, Poblet JM (2002) J Am Chem Soc 124:12574
9. Poblet JM, López X, Bo C (2003) Chem Soc Rev 32:297
10. López X, de Graaf C, Maestre JM, Bénard M, Bo C, Poblet JM (2005) J Chem Theor Comp 1:856
11. Fernández JA, López X, Bo C, de Graaf C, Baerends EJ, Poblet JM (2007) J Am Chem Soc 129:12244
12. Suaud N, Gaita-Ariño A, Clemente-Juan JM, Sánchez-Marín J, Coronado E (2002) J Am Chem Soc 124:15134
13. Suaud N, Gaita-Ariño A, Clemente-Juan JM, Sánchez-Marín J, Coronado E (2003) Polyhedron 22:2331
14. Suaud N, Gaita-Ariño A, Clemente-Juan JM, Coronado E (2004) Chem Eur J 10:4041
15. Calzado CJ, Clemente-Juan JM, Coronado E, Gaita-Ariño A, Suaud N (2008) Inorg Chem 47:5889
16. Andersson K, Malmqvist P-Å, Roos BO (1992) J Chem Phys 96:1218
17. Miralles J, Castell O, Caballol R, Malrieu J-P (1993) Chem Phys 172:33
18. Shaik S, Hiberty P (2007) A chemist's guide to Valence Bond theory. Wiley, New York
19. Hiberty P Leforestier C (1978) J Am Chem Soc 100:2012
20. Broer R, Nieuwpoort WC (1981) Chem Phys 54:291
21. Malrieu J-P, Maynau D (1982) J Am Chem Soc 104:3021
22. Epiotis ND, Larson JR, Eaton HL (1982) Lect Notes Chem 29:1
23. van Lenthe JH, Balint-Kurti GG (1983) J Chem Phys 78:5699
24. Hirao K, Nakano H, Nakayma K, Dupuis M (1996) J Chem Phys 105:9227
25. Thorsteinsson T, Cooper DL, Gerratt J, Karadakov PB, Raimondi M (1996) Theor Chim Acta 93:343

26. de Graaf C, Broer R, Nieuwpoort WC, Bagus PS (1997) Chem Phys Lett 272:341
27. Dijkstra F, van Lenthe JH, (2000) J Chem Phys 113:2100
28. Calzado CJ, Cabrero J, Malrieu J-P, Caballol R (2002) J Chem Phys 116:2728
29. Shaik S, Kumar D, de Visser SP (2008) J Am Chem Soc 130:10218
30. Bordas E, Caballol R, de Graaf C, Malrieu J-P (2005) Chem Phys 309:259
31. Perdew JP (1986a) Phys Rev B 33:8800
32. Perdew JP (1986b) Phys Rev B 34:7406
33. Becke AD (1986) J Chem Phys 84:4525
34. Becke AD (1988) Phys Rev A 38:3098
35. te Velde G, Bickelhaupt FM, Baerends EJ, Fonseca Guerra C, van Gisbergen SJA, Snijders JG, Ziegler T (2001) J Comp Chem 22:931
36. Adf 2005.01, Department of Theoretical Chemistry, Vrije Universiteit, Amsterdam
37. Becke AD (1993) J Chem Phys 98:5648
38. Lee CT, Yang WT, Parr RG (1988) Phys Rev B 37:785
39. Ahlrichs R, Bär M, Häser M, Horn H, Kölmel C (1989) Chem Phys Lett 162:165
40. Treutler O, Ahlrichs R (1995) J Chem Phys 102:346
41. Karlström G, Lindh R, Malmqvist P-Å, Roos BO, Ryde U, Veryazov V, Widmark P-O, Cossi M, Schimmelpfennig B, Neogrady P et al (2003) Comput Mater Sci 28:222
42. Ben Amor N, Maynau D (1998) Chem Phys Lett 286:211
43. Schäfer A, Huber C, Ahlrichs R (1994) J Chem Phys 100:5829
44. Roos BO, Lindh R, Malmqvist P-Å, Veryazov V, Widmark P-O (2005) J Phys Chem A 109:6575
45. Clemente-Léon M, Coronado E, Jiménez-Saiz C, Gómez-García CJ, Martínez-Ferrero E, Almeida M, Lopes EB (2001) J Mater Chem 11:2176
46. Allcock HR, Bissell EC, Shawl ET, (1972) J Am Chem Soc 94:8603
47. Fuchs J, Freiwald W, Hartl H (1978) Acta Crystallogr Sect B 34:1764
48. Pope MT, Müller A (1990) Angew Chem Int Ed 30:34
49. Clemente-Juan JM, Coronado E, Gaita-Ariño A, Suaud N, (2007) J Phys Chem A 111:9969
50. Angeli C, Cimiraglia R, Malrieu J-P (2008) J Chem Educ 85:150